Wearable Dual-Band Quasi-Yagi Antenna for UHF-RFID and 2.4 GHz Applications

Rajesh Kumar Singh, *Student Member, IEEE*, Andrea Michel, *Member, IEEE*, Paolo Nepa, *Senior Member, IEEE*, and Alfredo Salvatore

***Abstract*— A compact wearable dual-band quasi-Yagi RFID-reader antenna is designed for being incorporated into a smart glove. The antenna dual-band capability allows the integration of both the RFID reader at UHF band and a wireless data link at 2.4GHz, into a single compact and wearable device. Dipole and loop antennas are combined into a quasi-Yagi structure to be placed on a hand back, in order to detect tagged objects close to the hand palm and fingers, during the operator normal activities. The dual-band driven element consists of a rectangular-shaped folded dipole (resonating at the ETSI UHF RFID band, 865-868 MHz) and a rhombus-shaped folded dipole (resonating at the WLAN band, 2400-2485 MHz). A few parasitic elements (reflector and directors) are included to focus the field in the required direction, namely out of the worker's hand. A prototype of the proposed textile antenna is developed on a stretchable fabric and its performance is measured in terms of read range and near-field distribution, at 868 MHz, and radiation pattern and gain at 2.45 GHz.**

***Index Terms*—Compact antenna, dipole antenna, dual-band antenna, loop antenna, RFID technology, textile antenna, wearable antenna, Yagi-Uda antenna.**

I. Introduction

ULTRA High Frequency (UHF) Radio Frequency Identification (RFID) systems find applications in industrial and commercial sectors (electronic toll collection, libraries, animal tracking, security and healthcare) due to their attractive properties such as relatively high data rates, satisfactory read ranges and low implementation costs [1]-[5]. In several Internet-of-Things applications, UHF-RFID systems are combined with other wireless systems such as WLAN, Bluetooth and GPS, in order to develop worker tools with multiple functionalities. In this context, various dual-band antennas were investigated to limit the number of radiating elements as well as to reduce the volume occupied by the antenna inside the device [6]-[15]. Among others, dual-band antennas which operate at both UHF-RFID and 2.4 GHz bands (Bluetooth or 802.11b) have been designed as they allow the RFID reader to transmit collected data toward a management data center through a wireless local area network. Several approaches have been adopted to realize dual-band antennas. In [7], a sequential rotation feeding technique and a miniaturized circularly polarized (CP) patch are used to get a dual-band antenna for ETSI UHF RFID and for WLAN IEEE 802.11b,g applications. In [8]-[9], aperture-coupled two-layers antennas at UHF and microwave bands are developed. Dual-band operation is obtained in [10] by using an annular plate with curved and rectangular slots. A dual-band single-layer substrate diamond-shaped antenna has been presented in [11]. It has dimensions of 19×19×0.76 cm^3 and operates at UHF band (902-920MHz) and ISM band (2400-2500MHz); the size of the antenna is relatively large because of the air gap between the feed and the radiating element. A dual-band RFID antenna operating at 930 and 2450 MHz is presented in [12]; the antenna has three layers with a total height of 2.5 cm. In [13], a compact dual-band printed quadrifilar antenna for UHF RFID/GPS operations is presented, with an overall size of 6×6×0.9 cm^3. Antennas reported in [14]-[15] have good performance in both operating bands but are not suitable for wearable applications as they are printed on a thick substrate.

It is worth noting that UHF RFID technology has attracted attention in wearable applications where the reader and the antenna are placed close to the human body [16]-[23]. In the framework of the so-called smart gloves, UHF RFID tags or reader antennas are integrated into protective gloves which may help workers during their activities [19], [20], or which may help impaired people in daily life or during a rehabilitation process [21], [22].

Wearable antennas have been developed to support workers during their daily work, but there are challenges in producing such antennas while keeping the anticipated performance because the latter are affected by the presence of human body [23], [24]. Various low-profile wearable antennas have been reported for UHF RFID systems, and few of them were designed for smart gloves. Two cases have been described in the scientific literature to create glove integrated antennas: a bracelet antenna [25] or a

Manuscript received XXX

This work was supported in part by the Italian Ministry of Education and Research (MIUR) in the framework of the CrossLab project (Departments of Excellence)

R. K. Singh (corresponding author), A. Michel and P. Nepa are with the Department of Information Engineering, University of Pisa, Pisa, Italy (e-mail: rajesh.singh@dii.unipi.it; andrea.michel@unipi.it; paolo.nepa@unipi.it).

A. Salvatore is with Sensor ID, Campobasso, Italy (e-mail: alfredo.salvatore@sensorid.it).

printed antenna (on a hand back) [26], as shown in Fig. 1. To get a higher field strength without increasing the transmitted power, the number of turns of loop or solenoid antennas has to be increased, giving rise to more complex and non-planar structures. Moreover, in loop or solenoid antennas, the field is bi-directional and part of the radiated power is radiated toward the human arm, so reducing the antenna efficiency. Among others, Yagi-Uda antennas may

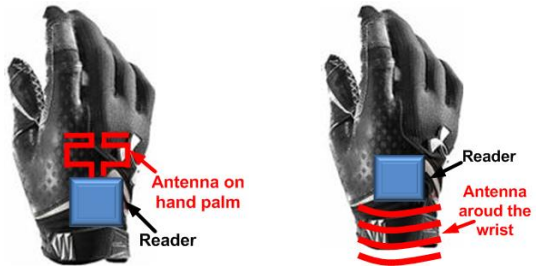

(a) (b)

Fig. 1 RFID antennas for smart gloves are typically designed (a) on hand back (b) around the wrist.

be effective to implement an end-fire radiation pattern [26], [27]. In this paper, a compact wearable dual-band quasi-Yagi reader antenna is proposed to be integrated onto the hand back of a smart glove for ETSI UHF RFID and WLAN (2.45GHz) applications, as they enable the glove-integrated RFID reader to transmit collected data toward a management data center through a wireless local area network (WLAN). Starting from the compact single-band UHF RFID quasi-Yagi antenna designed in [26], a second folded dipole has been added to also cover the WLAN frequency band at 2.45GHz. Since the tagged objects to be identified are close to the operator's hand, the tag lies in the reader antenna's near-field region [28]. On the other hand, the 2.4GHz antenna must have a satisfactory realized gain to reach the access point. The paper is organized as follows. The design of single- and dual-band versions of the quasi-Yagi antenna is introduced in Section II. Quasi-Yagi design with parasitic elements is discussed in Section III. Conclusions are summarized in Section IV.

II. Folded Dipole Antenna Design

A Yagi-Uda antenna consists of a single driven element, typically a dipole or a folded dipole, and parasitic elements operating as a reflector and directors. To come out with a dual-band quasi-Yagi antenna, a single-band quasi-Yagi antenna is designed first. The straight dipole shown in Fig. 2a and resonating at 868 MHz is folded in such a way that surface current flowing along its perimeter is in-phase, so that the excited magnetic field is almost uniform, and strong enough to detect tagged objects close to the hand palm. The perimeter of the fed dipole shown in Fig. 2b is lower than half a wavelength at the design frequency. An additional folded dipole (Fig. 2c) resonating at 2450 MHz is added to the original folded dipole. Surface currents on the folded dipole are plotted in Fig. 3, at 868 and 2450 MHz, confirming that the smallest folded dipole mainly gives its contribution at the higher band. The analysis of the folded dipole is done to understand its operation and near field distribution. Normally, element spacing in Yagi-Uda antennas is in the order of 0.13λ to 0.45λ; to reduce the size of the structure, the spacing can be reduced further and the elements can be meandered. As typical for wearable antenna design, the size of each part of the antenna has been optimized by taking into account the effects of body tissues. In particular, a multilayer human hand model has been included in the simulated scenario, as shown in Fig. 4. The assumed model for the hand consists of various hand-shaped finite layers representing the skin, fat, muscle and bone tissues [29], which are characterized through frequency dependent complex permittivities. Model parameters are discussed in [30], [31] and listed in Table I. Full-wave electromagnetic simulations have been carried out by means of CST Microwave Studio®.

The total length of one arm of the outer folded dipole (rectangular-shaped) is $2*L_1 + L_2 + L_3 + L_4 = 8.2$ cm, which is close to a quarter wavelength at 868 MHz (λ = 34.56 cm at 868 MHz, being λ the wavelength in free space).

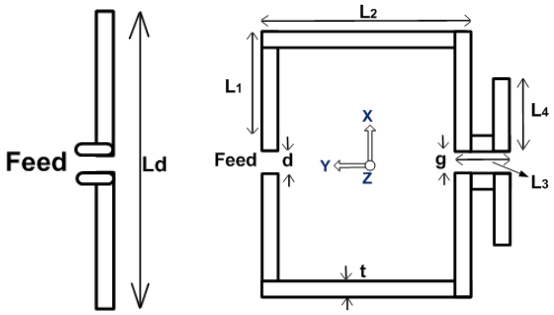

(a) (b)

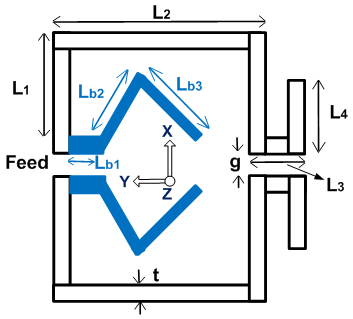

(c)

Fig.2 Design steps of a wearable dual-band folded dipole antenna (a) straight dipole (b) single-band folded dipole (c) dual-band folded dipole: Dimensions: L_d = 15.86 cm, L_1= 1.5 cm, L_2 = 3.5 cm, g = 0.2 cm d = 0.2 cm, L_3 = 0.6 cm, L_4 = 1.1 cm L_{b1} = 0.2 cm, L_{b2} = 1.3 cm, L_{b3} = 1.48 cm.

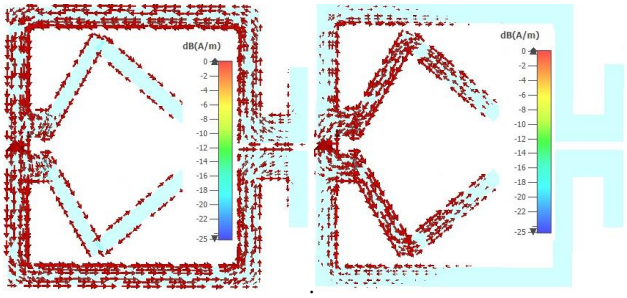

(a) (b)

Fig. 3 Normalized surface current on a wearable dual-band folded dipole antenna at (a) 868 MHz (b) 2450 MHz.

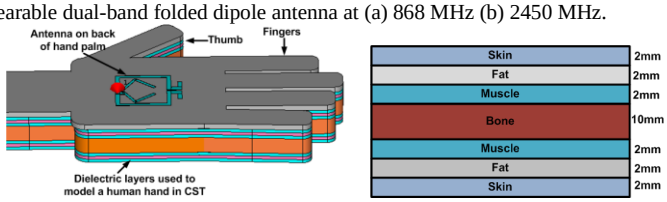

Fig. 4 Human hand model in numerical simulations.

Table 1: Dimensions and electrical properties of human hand model

Tissue layer	Thickness (mm)	Conductivity @ 868MHz (S/m)	Dielectric constant @ 868MHz	Conductivity @ 2450MHz (S/m)	Dielectric constant @ 2450MHz
Skin	2 mm	0.85	41	1.46	38
Fat	2 mm	0.05	5.46	0.1	5.3
Muscle	2 mm	0.93	55	1.74	52.73
Bone	10 mm	0.14	12.5	0.4	11.4

The length of one arm of the inner folded dipole (rhombus-shaped) is L_{b1} + L_{b2} + L_{b3} = 2.98 cm, which is close to a quarter wavelength at 2450 MHz (λ = 12.24 cm at 2450 MHz). The reflection coefficient of the single-band and dual-band folded dipoles are plotted in Fig. 5. From results in Fig. 6, it is apparent that the imaginary part crosses the zero-impedance line twice, for the dual-band folded dipole.

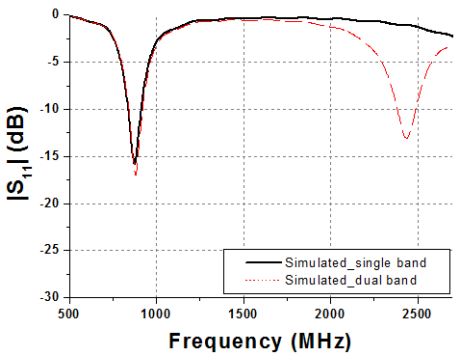

Fig. 5 Reflection coefficient of wearable single- and dual-band folded dipole antennas.

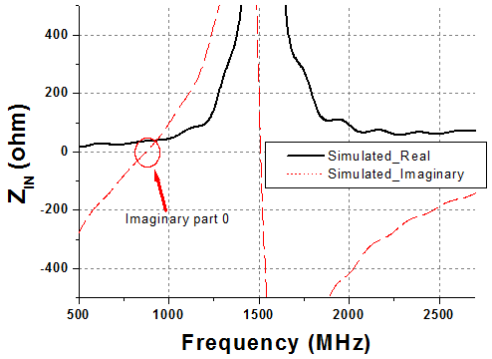

(a)

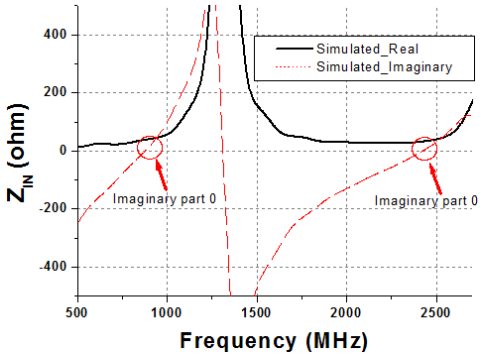

(b)

Fig. 6 Input impedance of (a) single-band folded dipole (b) dual-band folded dipole.

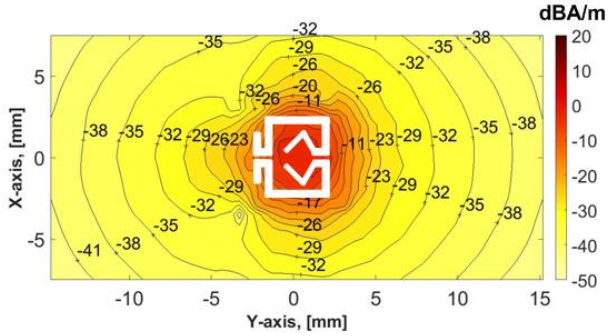

(a)

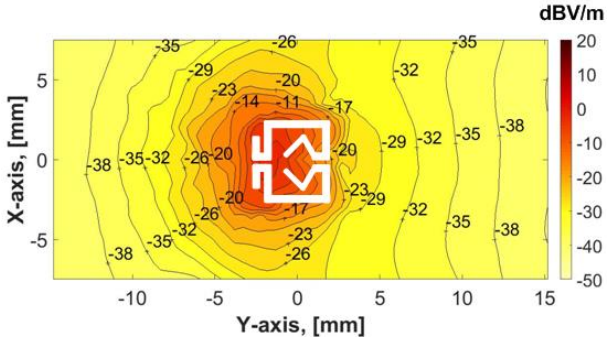

(b)

Fig. 7 Field distributions of quasi-Yagi structure on a XY-plane at z = 2.5 cm from the antenna surface, at 868 MHz (a) magnetic field (b) electric field. (1 A current is applied at the feeding port).

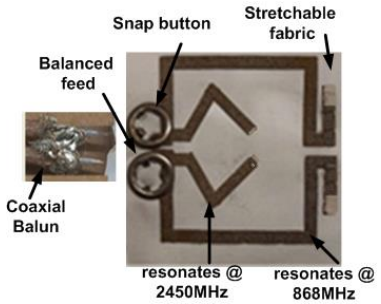

Fig. 8 Photograph of a prototype of the dual-band textile antenna.

The real part of the input impedance is close to 50Ω at 868 and 2450 MHz, which implies good impedance matching at both frequencies. It can also be seen from the reflection coefficients plot in Fig. 5 that the value of |S11| is less than -10 dB at 868 and 2450 MHz. Magnetic and electric field distributions in Fig. 7 are calculated on a XY-plane at a height of 2.5 cm (z = 2.5 cm) from the folded dipole surface. The magnitude of the magnetic field is almost uniform close to the folded dipole and field strengths (magnitude of electric and magnetic fields) exhibit almost the same amplitude along positive and negative directions of the y-axis. After analyzing the field strength and dual-band operation in the simulations, the proposed structure is fabricated on a stretchable fabric, as shown in Fig. 8. Resonance frequencies of the fabricated textile antenna shifts downward because of the finite sheet resistance (0.6 Ω/sq) of the textile material and finite thickness of the stretchable fabric. Antenna is slightly tuned by removing the conductive material at the end of the dipole arms to shift the resonance at 868 and 2450 MHz as shown in Fig. 8.

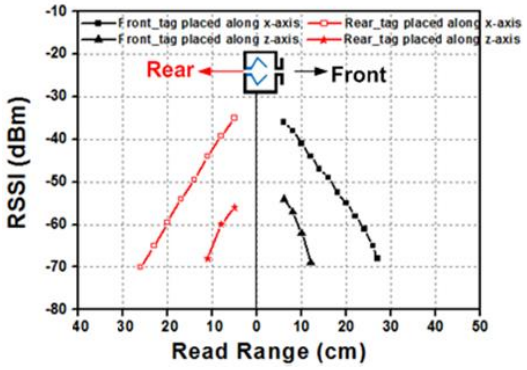

(a)

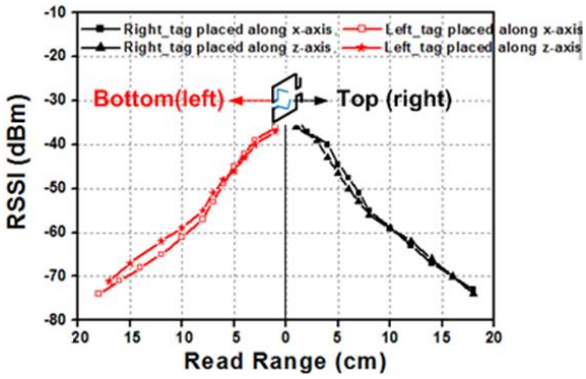

(b)

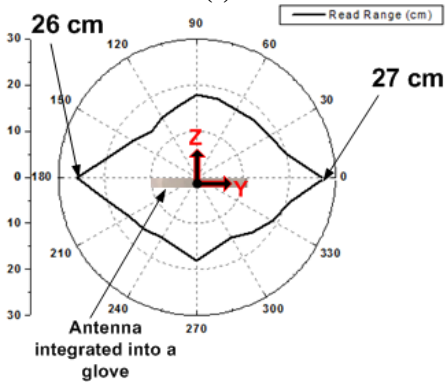

(c)

Fig. 9 Measured RSSI as a function of the distance (a) front and rear directions when a test dipole tag is placed along x-axis (co-pol case) or along z-axis (cross-pol case) (b) top and bottom directions when dipole tag is placed along x- and z-axis, (c) read ranges in various directions from the structure.

Another prototype made with copper tape is fabricated on the same stretchable fabric, and then measured. The performance of copper tape and textile antennas are quite comparable in the near-field at 868 MHz, as well as in the far-field at 2450 MHz. On the other hand, there are advantages of textile antenna over copper tape one, as the textile antenna is more durable compared to copper tape antenna. Also, textile antenna provides resistant to shock and vibrations. RF performance of the textile antenna does not deteriorate after repetitive flexing or bending. Here, a textile antenna is fabricated using a plain fabric as shown in Fig. 8. Normally, antennas for smart gloves are made of conductive threads or by plating a non-conductive fabric with metal or alloy. Here, metallic parts are made on a stretchable fabric. A quadri-elastic plain conductive fabric has been used. Fabric is based on silver yarn woven with Lycra. This plain fabric allows better stability of antenna parameters, but it exhibits a low conductivity. The conductive yarn has been cut with laser machine, and then the textile antenna has been integrated into the glove fabric by means of thermo-adhesivation. To feed the textile antenna, snap buttons are attached to it instead of soldering. Indeed, it is not possible to solder such antenna made on a stretchable fabric or any other textile material. Textile antenna is then connected to a commercial RFID reader (CAEN ION) through a balun. A linearly polarized tag (LAB ID UH100) is used to collect the values of the Received Signal Strength Indicator (RSSI) and estimate the read range, when the reader transmitted power is 44.6 mW (16.5 dBm). RSSI is measured in various directions (front, rear, top, and bottom) by placing the dipole tag along x-axis (co-polarized with the reader antenna) and along z-axis (cross-polarized with respect to the reader antenna), as shown in Fig. 9 (a) and (b). Fig. 9 (c) shows the read range in various directions away from the structure. The tag ID is detected at larger distances in front and rear directions when dipole tag is placed along x-axis because the polarization matching condition is met. Along top and bottom directions, the tag ID is detected at almost similar distances (up to 18cm), because it is irrespective of the alignment of the dipole tag, being the magnetic field strong enough at those directions.

The aim of making this design is to detect tagged objects close to the hand and reduce radiation along other directions. For this reason, we need higher field strength close to the hand palm and along the hand fingers. Rectangular-shaped folded dipole has strong magnetic field close to the hand palm at 868 MHz as seen in Fig. 7. To get higher field strength along the hand fingers, a Yagi-like structure is needed; it can be done by adding parasitic elements to this dual-band folded dipole, as discussed in the next section.

III. Quasi-Yagi Design with Parasitic Elements

One reflector and two directors are added to the original folded dipole structure. Lengths, shapes of the Yagi elements and their spacing are the key parameters of the design. Optimized dimensions of the proposed design are listed in Table II. When parasitic elements are added to the folded dipole, operating frequencies are shifted downwards because of the loading effect of the parasitic elements. Conductive material at the end of dipole arm is further removed to get back to the original frequencies. The final geometry and photograph of the quasi-Yagi antenna are shown in Fig. 10.

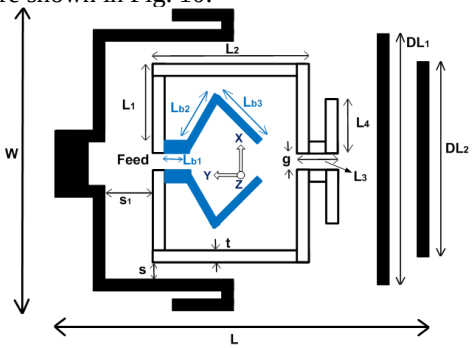

(a)

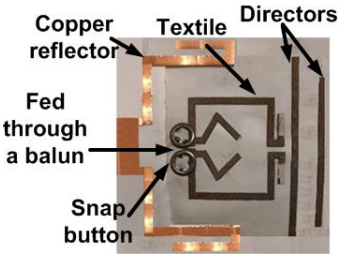

(b)

Fig. 10 Proposed compact and wearable dual-band quasi-Yagi antenna with reflector and two directors (a) geometry (b) photograph of a prototype.

Table II: Proposed antenna dimensions

Parameter	Value (cm)	Parameter	Value (cm)
DL_1	4.8	L_{b1}	0.2
DL_2	4.2	L_{b2}	1.3
L	6.5	L_{b3}	1.48
L_1	1.5	s	0.5
L_2	3.5	s_1	1.8
L_3	0.6	t	0.3
L_4	0.6	W	6.0

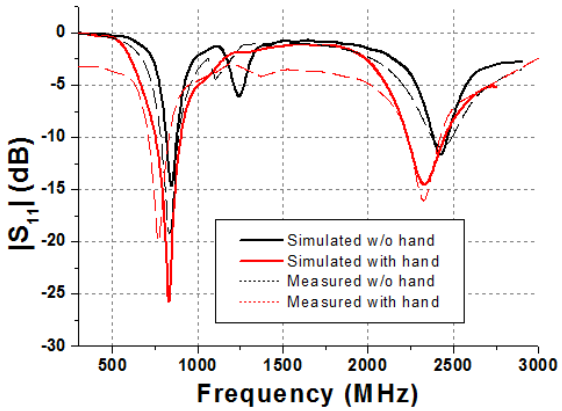

Fig. 11 Simulated and measured reflection coefficients of a wearable dual-band quasi-Yagi antenna.

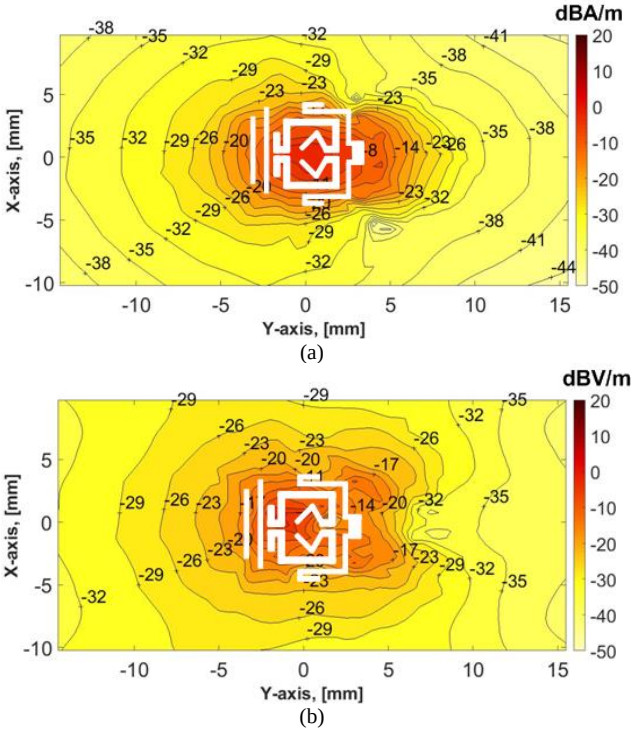

Fig. 12 Field distributions of quasi-Yagi antenna on a XY-plane at z = 2.5 cm at 868 MHz (a) magnetic field (b) electric field. (1 A current is applied at the feeding port).

Both simulated and measured reflection coefficients are shown in Fig. 11, when the antenna is integrated into the glove, with and without the presence of the hand. Human hand model shown in Fig. 4 has been included in the simulated environment. The presence of the human hand causes a shift of the resonance toward lower frequencies, as expected since the human body is a high permittivity medium. The adopted hand model [30] leads to a quite good agreement between simulation and measurement results.

Magnetic and electric field distributions on a XY-plane at a height of 2.5 cm (z = 2.5 cm) is shown in Fig. 12. The magnitude of electric and magnetic fields is larger along negative y-axis (along the hand fingers).

In a practical use of the smart glove, the textile antenna may be subject to bending due to the hand movement (e.g. opening and closing hand actions). The bending and stretching of the antenna may cause a variation of the distance between antenna elements,

thus affecting its performance. A study of bending is done by means of numerical simulations. Specifically, the proposed antenna with the hand model has been bent on a cylindrical surface of radius R, as schematically represented in Fig. 13. Reflection coefficients for various values of *R* are plotted in Fig. 14 to show the bending effects. Hand bending does not affect much the performance of antenna in terms of reflection coefficient. A decrease of about 0.6dB on the realized gain toward the hand's fingers is estimated when R=8cm (closing hand) with respect to the straight hand (opening hand). Measured RSSI and read ranges at 868 MHz are plotted in Fig. 15. Adding the parasitic elements determines an enhancement of 7 cm in the reading range along hand fingers and advantageous reduction of 10 cm along the arm, as seen when comparing results in Fig. 9(c) and 15(c).

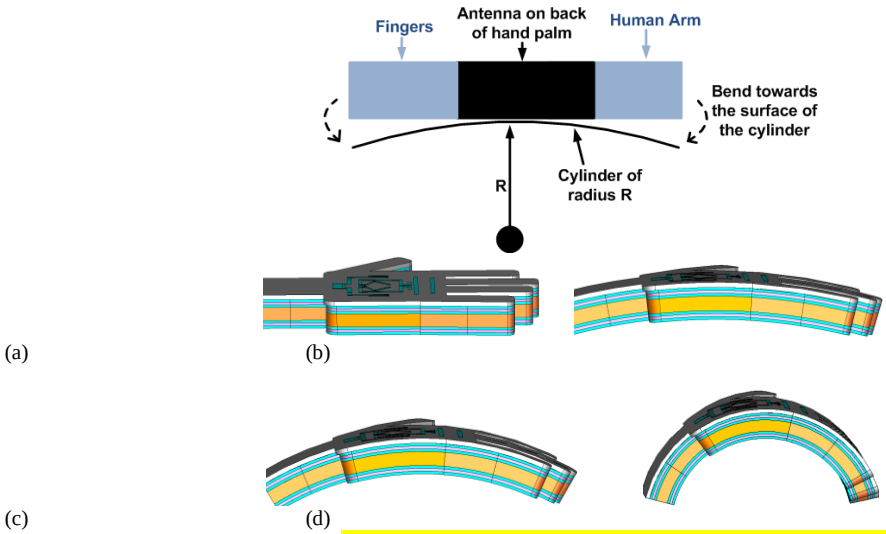

Fig. 13 Simulated antenna in CST Microwave Studio when it is bent over a cylinder (a) R = ∞ (no bending, corresponding to an open hand) (b) R = 40 cm (c) R = 20 cm (d) R = 8 cm (corresponding to an almost closed hand).

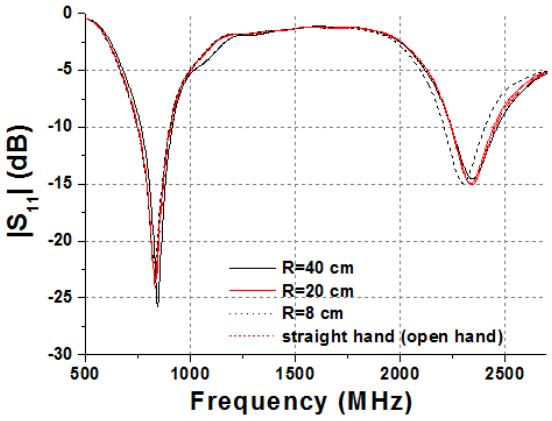

Fig. 14. Simulated reflection coefficients considering straight and bending hand, for different values of the cylinder radius.

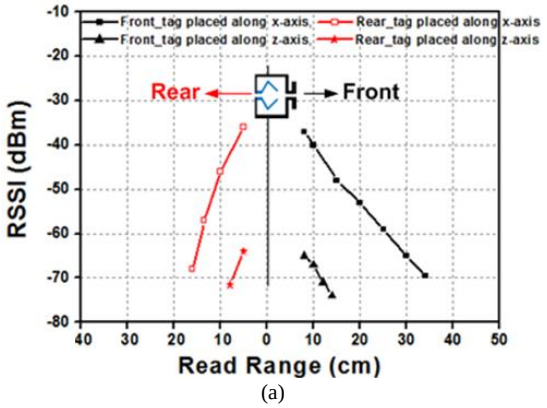

(a)

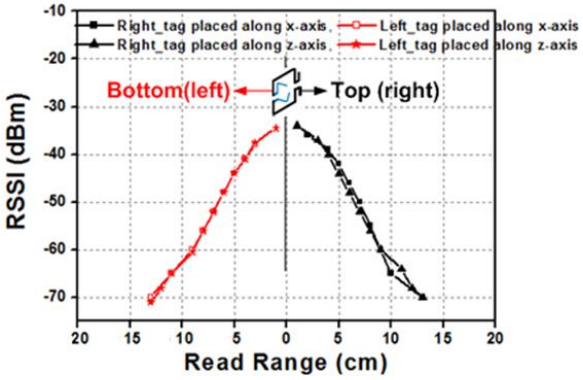

(b)

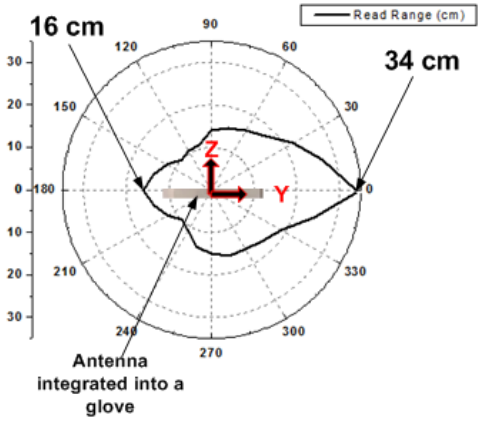

(c)

Fig. 15 Measured RSSI as a function of the distance (a) front and rear directions, when a test dipole tag is placed horizontally (along x-axis, co-pol case) or vertically (along z-axis, cross-pol case) (b) top and bottom directions when dipole tag is placed along x- and z-axis, (c) read range in various directions from the structure.

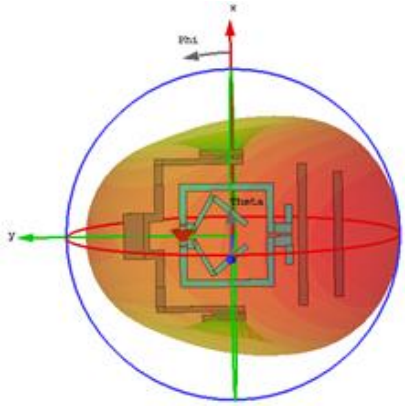

Fig. 16 Simulated 3D radiation pattern at 2450 MHz.

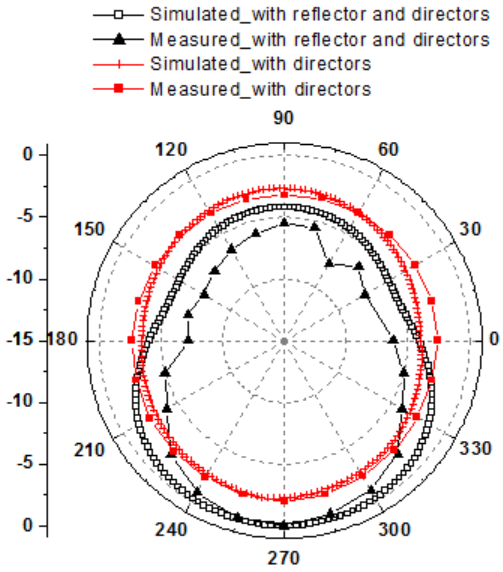

(a)

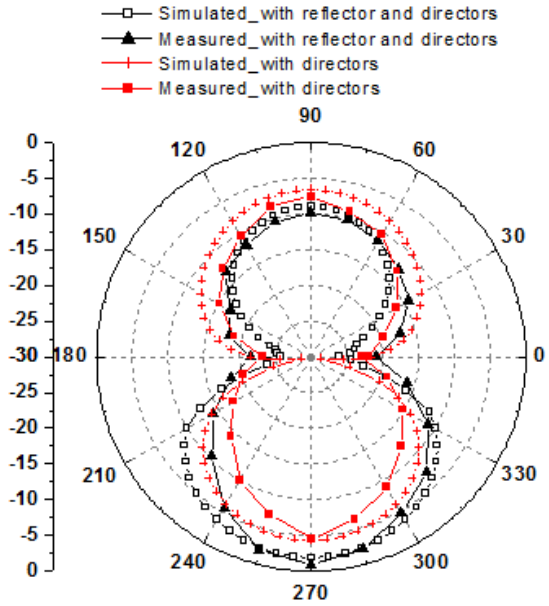

(b)

Fig. 17 Simulated and measured radiation patterns of a wearable dual-band quasi-Yagi antenna at 2450 MHz. (a) H-plane (b) E-plane

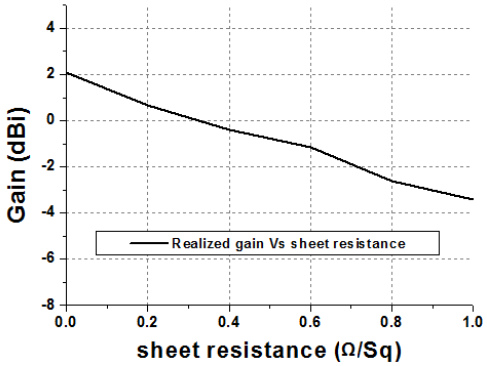

Fig. 18 Simulated realized gain with different value of sheet resistance of a conductive material.

Since tags must be detected in proximity of the reader antenna (antenna near-field region), the radiation pattern at UHF RFID band is not a key performance indicator. On the other hand, at WLAN band, the antenna operates in the far-field region. Thus, in Fig.

16, the simulated 3D radiation pattern of the antenna at the frequency of 2450MHz is shown (when the glove is not worn). In Fig. 17, simulated and measured radiation patterns on the two principal planes are plotted at 2450 MHz. The H-plane (YZ plane) pattern is shown in Fig 17(a); it is possible to see that the H-plane pattern of antenna with only directors is not omnidirectional. Specifically, the front-to-back ratio is 1.3dB and 1.8dB from simulation and measurement results, respectively, which may be increased by introducing more directors. However, by increasing the number of directors, antenna size increases too, resulting in an obtrusive structure to be integrated onto a glove. On the other hand, the presence of a reflector can further focus radiated field toward the front direction. In this case, front-to-back increases up to 4.35dB and 5.5dB for simulation and measurement results, respectively, as shown in Fig. 17(a). Similar considerations apply to the E-Plane (XY plane) pattern plotted in Fig. 17(b). Generally speaking, the radiation patterns differ from the theoretical patterns of a Yagi-Uda antenna due to the folded and meandered structure of the antenna elements. As an example, for a typical Yagi-Uda antenna composed by dipoles, a null would be expected along the x-axis. For the proposed antenna layout, the null is not obtained due to the asymmetric layout of the folded structure. However, a minimum of the radiation pattern can be still observed along the x-axis, confirming the Yagi-like radiation pattern.

Measured realized gain of the textile antenna is -2.1 dBi while the simulated is -1.4 dBi. Reduction in the measured realized gain is due to the approximated characterization of the human hand tissues. Realized gain also depends on the material used during the fabrication process. Gain is analyzed by applying different sheet resistance values to the conductive material model. Larger the sheet resistance smaller the antenna gain, as it can be seen from Fig. 18. If an ideal lossless material is used in the simulations (vanishing sheet resistance), the simulated realized gain is 2.03 dBi, so confirming that the conductive material significantly affects the antenna gain.

IV. Conclusion

A compact wearable dual-band quasi-Yagi reader antenna is proposed in this paper to be integrated into smart gloves, on the hand back. The proposed dual-band textile structure was made on a stretchable fabric. Read range performance has been measured using COTS RFID reader and a tag at 868 MHz, while radiation patterns were measured at 2450 MHz. Performance of two quasi-Yagi structures (with and without parasitic elements) was compared in terms of read range; an enhancement of 7 cm in the reading range along hand fingers and a reduction of 10 cm along the arm was obtained. Also, the required directional property of the radiation pattern at 2450 MHz was achieved using parasitic elements. The proposed structure is planar and compact in size, as it can easily be fitted on a hand back.

References

[1] A. Pratelli, M. Petri, A. Farina, and M. Lupi, “Improving Bicycle Mobility in Urban Areas Through ITS Technologies: The SaveMyBike Project”, Advanced Solutions of Transport Systems for Growing Mobility, Sierpiński G. (eds) TSTP 2017, Advances in Intelligent Systems and Computing, vol 631. Springer, Cham

[2] L. Catarinucci et al., “An IoT-Aware Architecture for Smart Healthcare Systems,” in *IEEE Internet of Things Journal*, vol. 2, no. 6, pp. 515-526, Dec. 2015.

[3] A. S. Andrenko, "Optimized near-field antenna for UHF RFID smart shelf applications," 2015 IEEE International Symposium on Antennas and Propagation & USNC/URSI National Radio Science Meeting, Vancouver, BC, 2015, pp. 1576-1577.

[4] A. Buffi, A. Michel, P. Nepa and B. Tellini, "RSSI Measurements for RFID Tag Classification in Smart Storage Systems," in *IEEE Transactions on Instrumentation and Measurement*, vol. 67, no. 4, pp. 894-904, April 2018.

[5] S. Amendola, R. Lodato, S. Manzari, C. Occhiuzzi and G. Marrocco, "RFID Technology for IoT-Based Personal Healthcare in Smart Spaces," in *IEEE Internet of Things Journal*, vol. 1, no. 2, pp. 144-152, April 2014.

[6] Q. Liu, J. Shen, H. Liu and Y. Liu, "Dual-Band Circularly-Polarized Unidirectional Patch Antenna for RFID Reader Applications," in *IEEE Transactions on Antennas and Propagation*, vol. 62, no. 12, pp. 6428-6434, Dec. 2014.

[7] R. Caso, A. Michel, M. Rodriguez-Pino and P. Nepa, "Dual-Band UHF-RFID/WLAN Circularly Polarized Antenna for Portable RFID Readers," in *IEEE Transactions on Antennas and Propagation*, vol. 62, no. 5, pp. 2822-2826, May 2014.

[8] X. Zhishu and L. Xiuping, “Aperture coupling two-layered dual-band RFID reader antenna design,” in Proc. Int. Conf. on Microwave and Millimeter Wave Technology (ICMMT), Apr. 2008, vol. 3, pp. 1218–1221.

[9] F. Y. Kuo, P. H. Pan, C.-Y. Chiang, H. T. Hsu, and H. T. Chou, “Dual band aperture-coupled patch antenna for RFID mobile terminal applications,” in Proc. Asia-Pacific Microwave Conf. (APMC), Dec. 2010, pp. 2201–2204.

[10] C. Phongcharoenpanich and R. Suwalak, “Dual-band RFID-reader antenna using annular plate with curved and rectangular slots,” in Proc. Int. Conf. on Electromagnetics in Advanced Applications (ICEAA), 2010, pp. 633–636.

[11] M. I. Sabran, S. K. A. Rahim, A. Y. A. Rahman, T. A. Rahman, and M. Nor Evizal, “A dual-band diamond-shaped antenna for RFID application,” *IEEE Antennas Wireless Propag. Lett.*, vol. 10, pp. 979–982, 2011.

[12] Z. Xing, K. Wei, L. Wang and J. Li, "Dual-band RFID antenna for near field of 0.93 GHz and far field of 2.45 GHz," *2016 IEEE 5th Asia-Pacific Conference on Antennas and Propagation (APCAP)*, Kaohsiung, 2016, pp. 453-454.

[13] K. Oh, W. Son, S. Cha, M. Lee and J. Yu, "Compact Dual-Band Printed Quadrifilar Antennas for UHF RFID/GPS Operations," in *IEEE Antennas and Wireless Propagation Letters*, vol. 10, pp. 804-807, 2011.

[14] H.-Y. A. Yim, C.-P. Kong, and K.-K. M. Cheng, “Compact circularly polarised microstrip antenna design for dual-band applications,” *Electronics Letters*, vol. 42, no. 7, pp. 380-381, 2006.

[15] M. Taouzari, J. E. Aoufi, A. Mouhsen, H. Nasraoui and O. E. Mrabat, "900 MHz and 2.45 GHz compact dual-band circularly-polarized patch antenna for RFID application," *2015 Conference on Microwave Techniques (COMITE)*, Pardubice, 2015, pp. 1-4.

[16] X. Chen *et al*., "Electro-textile glove-tags for wearable RFID applications," *2017 International Symposium on Antennas and Propagation (ISAP)*, Phuket, 2017, pp. 1-2.

[17] S. Ahmed, S. M. M. Rehman, L. Ukkonen and T. Björninen, "Glove-Integrated Slotted Patch Antenna for Wearable UHF RFID Reader," *2018 IEEE International Conference on RFID Technology & Application (RFID-TA)*, Macau, 2018, pp. 1-5.

[18] C. Scheuermann, M. Strobel, B. Bruegge and S. Verclas, "Increasing the Support to Humans in Factory Environments Using a Smart Glove: An Evaluation," *2016 Intl IEEE Conferences on Ubiquitous Intelligence & Computing, Advanced and Trusted Computing, Scalable Computing and Communications, Cloud and Big Data Computing, Internet of People, and Smart World Congress*, Toulouse, 2016, pp. 847-854.

[19] S. Ahmed, S. T. Qureshi, L. Sydänheimo, L. Ukkonen and T. Björninen, "Comparison of Wearable E-Textile Split Ring Resonator and Slotted Patch RFID Reader Antennas Embedded in Work Gloves," in *IEEE Journal of Radio Frequency Identification*, vol. 3, no. 4, pp. 259-264, Dec. 2019.

[20] Z. Khan et al., "Glove-Integrated Passive UHF RFID Tags—Fabrication, Testing and Applications," in *IEEE Journal of Radio Frequency Identification*, vol. 3, no. 3, pp. 127-132, Sept. 2019.

[21] G. Marrocco, "RFID Antennas for the UHF Remote Monitoring of Human Subjects," in *IEEE Transactions on Antennas and Propagation*, vol. 55, no. 6, pp. 1862-1870, June 2007.

[22] D. Devipriya, V. S. Sri and I. Mamatha, "Smart Store Assistor for Visually Impaired," 2018 International Conference on Advances in Computing, Communications and Informatics (ICACCI), Bangalore, 2018, pp. 1038-1045.

[23] A. Michel et al., "Design Considerations on the Placement of a Wearable UHF-RFID PIFA on a Compact Ground Plane," in *IEEE Transactions on Antennas and Propagation*, vol. 66, no. 6, pp. 3142-3147, June 2018.

[24] G. A. Casula, A. Michel, P. Nepa, G. Montisci and G. Mazzarella, "Robustness of Wearable UHF-Band PIFAs to Human-Body Proximity," in *IEEE Transactions on Antennas and Propagation*, vol. 64, no. 5, pp. 2050-2055, May 2016.

[25] M. Daiki and E. Perret, "Segmented Solenoid Coil Antenna for UHF RFID Near-Field Reader Applications," in *IEEE Journal of Radio Frequency Identification*, vol. 2, no. 4, pp. 210-218, Dec. 2018.

[26] R. K. Singh, A. Michel, P. Nepa and A. Salvatore, "Design of a Compact Yagi-Uda Antenna for Near Field UHF RFID Smart gloves," *2019 IEEE International Conference on RFID Technology and Applications* (RFID-TA), Pisa, Italy, 2019, pp. 453-457.

[27] P. V. Nikitin and K. V. S. Rao, "Compact Yagi antenna for handheld UHF RFID reader," *2010 IEEE Antennas and Propagation Society International Symposium*, Toronto, ON, 2010, pp. 1-4.

[28] A. Michel, P. Nepa, X. Qing, and Z. N. Chen, "Considering high performance near-field reader antennas: Comparisons of proposed antenna layouts for ultrahigh-frequency near-field radio-frequency identification," *IEEE Antennas Propag. Mag.*, vol. 60, no. 1, pp. 14–26, Feb. 2018.

[29] A. Michel, K. Karathanasis, P. Nepa and J. L. Volakis, "Accuracy of a Multiprobe Conformal Sensor in Estimating the Dielectric Constant in Deep Biological Tissues," in IEEE Sensors Journal, vol. 15, no. 9, pp. 5217-5221, Sept. 2015.

[30] S. Ahmed, A. Mehmood, L. Sydänheimo, L. Ukkonen and T. Björninen, "Glove-Integrated Textile Antenna with Reduced SAR for Wearable UHF RFID Reader," *2019 IEEE International Conference on RFID Technology and Applications (RFID-TA)*, Pisa, Italy, 2019, pp. 231-235.

[31] IT'IS Foundation, Tissue Properties [Online]. Available: https://itis.swiss/virtual-population/tissue-properties/downloads/

Rajesh Kumar Singh received the B.Tech. degree in electronics and communication engineering from Uttar Pradesh Technical University, Lucknow, India in 2010 and M.Tech. degree in microwave electronics from Delhi University South Campus, Delhi, India in 2013. He received the Ph.D. degree in microwave engineering from the Indian Institute of Technology, Delhi, India in 2018. He is currently a Post-Doctoral Researcher at the Microwave and Radiation Laboratory, Department of Information Engineering, University of Pisa, Pisa, Italy. His current research interests include the design of reconfigurable antennas for communication systems, and glove integrated antennas for near field UHF-RFID readers. He served as a chairman for the years 2016-2018 and treasurer for the years 2014-2016 of IEEE Student Branch Chapter of Indian Institute of Technology Delhi, India.

Andrea Michel (S'08-M'15) received the B.E., M.E. (summa cum laude), and Ph.D. degrees in telecommunications engineering from the University of Pisa, Pisa, Italy, in 2009, 2011, and 2015, respectively. In 2014, he was a Visiting Scholar with the Electro Science Laboratory, The Ohio State University, Columbus, OH, USA. During this period, he was involved in research on a theoretical analysis on the accuracy of a novel technique for deep tissue imaging. Since 2015, he has been a Post-Doctoral Researcher in Applied Electromagnetism at the Microwave and Radiation Laboratory, Department of Information Engineering, University of Pisa, where he is currently an Assistant Professor. He is involved in the design of antennas for automotive applications, MIMO systems, and wearable communication systems, in collaboration with other research institutes and companies. His current research interests include the design of integrated antenna for communication systems and smart antennas for near field UHF-RFID readers. Dr. Michel was a recipient of the Young Scientist Award from the International Union of Radio Science, Commission B, in 2014, 2015, and 2016. In 2016, he received the Best Paper Honorary Mention from the IEEE International Conference on RFID Technology and Applications, Shunde, Guangdong, China. He serves as Early Career Representative for URSI Commission B (Fields and Waves).

Paolo Nepa (SM '20) received the Laurea degree (summa cum laude) in electronics engineering from the University of Pisa, Pisa, Italy, in 1990. Since 1990, he has been with the Department of Information Engineering, University of Pisa, where he is currently a Full Professor. In 1998, he was a Visiting Scholar at the Electro Science Laboratory (ESL), The Ohio State University (OSU), Columbus, OH, USA, where he was involved in efficient hybrid techniques for the analysis of large antenna arrays. His current research interests include the design of wideband and multiband antennas, and antennas optimized for near-field coupling and focusing. In the context of UHF-RFID systems, he is working on techniques for radiolocalization of either tagged objects or

readers. He has coauthored more than 300 international journal articles and conference contributions. Dr. Nepa is a member of the Technical Advisory Board of URSI Commission B - Fields and Waves. He served as the General Chair of the IEEE RFID-TA 2019 International Conference. Since 2016, he has been serving as an Associate Editor for the IEEE Antennas and Wireless Propagation Letters. He was a recipient of the Young Scientist Award from the International Union of Radio Science, Commission B, in 1998.

Alfredo Salvatore, CEO of Sensor ID, got a Master Degree in Telecommunication Engineering "Cum Laude" in 2007. He was visitor research scholar at University of California Irvine working on definition of routing algorithms for distributed Wireless Sensor Networks. He was in Telecom Italia Research Laboratory working on WiMax terminals analysis and integration into Telecom Italia network mobile platform.He has expertise in wireless technology standard integration and implementation and in wireless network topology design. He has more than 10 years of experience in design, development and integration of devices based on proximity wireless technology for different kind of application such identification, payment, sensor data collecting, etc. In 2010 he founded Sensor ID, an electronic company that built a complete portfolio of embedded electronic modules based on IoT technologies like NFC, UHF RFID, Bluetooth, Nb-Iot, LoRA. So he worked on implementation of the functionalities required by standards on ARM based microcontroller. He has a strong knowledge of main microcontroller architectures and the main RF transceiver for RFID and wireless sensor network application provided by main silicon vendors. He was involved in several research and development project regarding integration of RFID and technology in different application scenario such as automotive (with for example FIAT Research Center, TRW, Denso, Lamborghini), access control and security with (for example ISEO Serrature, Tenaris), biomedical, building automation and process control (ex. Luxottica).